American Mineralogist, Volume 97, pages 1764–1770, 2012

High-pressure structural studies of eskolaite by means of single-crystal X-ray diffraction

Anastasia Kantor,[1,2,*] Innokenty Kantor,[2] Marco Merlini,[3] Konstantin Glazyrin,[1] Clemens Prescher,[1] Michael Hanfland,[2] and Leonid Dubrovinsky[1]

[1]Bayerisches Geoinstitut, Universität Bayreuth, D-95440 Bayreuth, Germany
[2]European Synchrotron Radiation Facility, BP 220, 38043 Grenoble, CEDEX 9, France
[3]Universita degli Studi di Milano, Dipartimento di Scienze della Terra, Via Botticelli 23, 20133 Milano, Italy

Abstract

The structural behavior of Cr_2O_3 was investigated up to ~70 GPa using single-crystal X-ray diffraction under a quasi-hydrostatic pressure (neon pressure medium) at room temperature. The crystal structure remains rhombohedral with the space group $R\bar{3}c$ (No. 167) and upon compression the oxygen atoms approach an ideal hexagonal close-packing arrangement. An isothermal bulk modulus of Cr_2O_3 and its pressure derivative were found to be 245(4) GPa and 3.6(2), respectively, based on a third-order Birch-Murnaghan equation of state and $V_0 = 288.73$ Å^3. An analysis of the crystal strains suggest that the non-hydrostatic stresses can be considered as negligible even at the highest pressure reached.

Keywords: High pressure, crystal structure, eskolaite

Introduction

For many decades X_2O_3 transition metals oxides attracted an interest of solid-state physicists, chemists, and geoscientists. Their electronic, magnetic, and structural properties made them a subject of many theoretical and experimental investigations. Like many others, Cr_2O_3 (chromia, mineral name eskolaite) was studied mostly as a powder (Sato and Akimoto 1979; Shim et al. 2004; Rekhi et al. 2000; Mougin et al. 2001) partially due to difficulty of the synthesizing single crystals of chromia, but mostly due to limitations of single-crystal X-ray diffraction studies at high pressures (Dubrovinsky et al. 2010).

At ambient conditions, chromium (III) oxide adopts the corundum type crystal structure with space group $R\bar{3}c$. The crystal structure consists of a hexagonal close-packed framework of oxygen anions with 2/3 of the octahedral voids occupied by chromium. In the *a*-*b* plane, CrO_6 octahedra form a so-called corundum-type pattern with each filled octahedron sharing common edges with three others (Fig. 1). Along the *c*-axis these layers alternate in such a way that each octahedron shares one common face with another.

The exact high-pressure phase diagram of Cr_2O_3 remains unclear, despite several studies. Due to slow kinetics of phase transformations of dense oxides, it is quite difficult to study the equilibrium phase relations at low and moderate temperatures and high pressures. It was predicted from first-principles calculations (Dobin et al. 2000) that at high pressures (above 15 GPa) Cr_2O_3 should transform from the hexagonal corundum-type structure to the orthorhombic Rh_2O_3-II type structure. Subsequently, this phase transition was confirmed by Shim et al. (2004), but at higher pressure (~30 GPa) and only after laser heating. However, their powder X-ray diffraction spectra of the high-pressure chromia phase at the same time can be interpreted as a perovskite-type orthorhombic structure (Shim et al. 2004), which is also very common among ternary transition metal oxides.

Another possible phase transition at lower pressures (13–15 GPa) and room temperature was reported based on the experimental observations by means of Raman scattering (Mougin et al. 2001; Shim et al. 2004), resistivity measurements (Minomura and Drickamer 1963) and X-ray diffraction (Shim et al. 2004). Significant broadening of some of the Raman and X-ray diffraction peaks was interpreted as a distortional transition from the hexagonal space group $R\bar{3}c$ to the monoclinic space group *I*2/*a* structure. These studies were performed on powdered samples under highly non-hydrostatic conditions, which make the detailed structural analysis of a monoclinic high-pressure phase nearly impossible. We, therefore, decided to reinvestigate the high-pressure behavior of Cr_2O_3 by means of single-crystal micro-diffraction at high pressures up to 70 GPa. In fact, this technique has been recently upgraded and it allows extracting very accurate structural information at the most extreme conditions (Dubrovinsky et al. 2010) and even after first- and second-order phase transitions (Merlini et al. 2012). When the present manuscript was in preparation another independent single-crystal study of Cr_2O_3 was published (Dera et al. 2011); the authors reported no structural phase transition up to 55 GPa at room temperature.

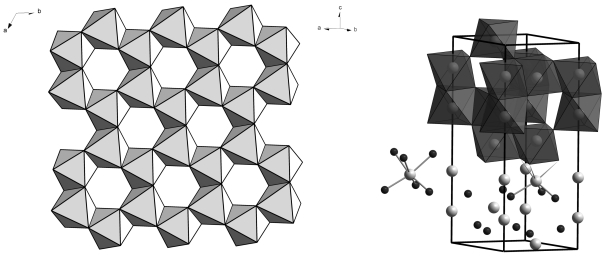

Figure 1. "Corundum" layer of CrO_6-octahedra (on the **left**). Every third octahedral in the layer is empty. On the **right**: Cr_2O_3 crystal structure. Light and dark gray spheres are chromium and oxygen atoms, respectively.

* E-mail: anastasia.kantor@uni-bayreuth.de

0003-004X/12/0010–1764$05.00/DOI: http://dx.doi.org/10.2138/am.2012.4103

EXPERIMENTAL TECHNIQUES

Single crystals of Cr_2O_3 were synthesized at 22 GPa and 1950 °C using commercially available Cr_2O_3 powder (99.999% purity, from Johnson Matthey Alfa Products). The synthesis procedure, along with the preliminary Raman and X-ray diffraction results, are described in the recent paper by Ovsyannikov and Dubrovinsky (2011). A selected Cr_2O_3 single crystal of 30 × 30 × 15 μm^3 was loaded in a 100 μm hole of an indented rhenium gasket along with several ruby spheres for quick pressure determination (Mao et al. 1986). Neon was loaded into the sample chamber at 1.4 kbar and used as a pressure-transmitting medium and as an internal pressure standard (Fei et al. 2007). Pressure was determined with a maximum uncertainty of 0.5 GPa at the highest pressure reached, based on the uncertainty of Ne lattice parameter determination. A symmetrical screw-driven piston-cylinder diamond-anvil cell (DAC) BX-90 (Kantor et al., in review) was employed for the current compressibility measurements. The cell was equipped with the Boehler-Almax design conical diamond anvils (Boehler and Hantsetters 2004) that give a full 80° 4θ X-ray aperture.

The X-ray diffraction (XRD) experiment was performed at the ID-09a beamline of the European Synchrotron Radiation Facility (ESRF). Data were collected at room temperature using the MAR555 flat panel detector mounted at about 310 mm apart from the sample and using a monochromatic (λ = 0.4148 Å) X-ray beam of about 10 × 10 μm^2 FWHM size. At each pressure point 160 frames in the ω-scanning range of –40° to +40° were collected (0.5° scanning step size) with an exposure time of one second. Around 400 Bragg reflections were detected at each pressure, among which around 70 were unique (Table 1). The data were processed using the CrysAlis software (Oxford Diffraction 2006). Crystal structure refinements using the integral intensities were carried out with the SHELXL-97 WinGX version (Sheldrick 2008), resulting in $R1$-factors between 3 and 5% (see Table 1). These values are typical for single-crystal X-ray diffraction analysis, but for the first time this method was expanded to ~70 GPa for Cr_2O_3. Such a high data quality is guaranteed not only by an advanced detector, but by a high coverage of a reciprocal space in the DAC. As an example, Figure 2 shows a reconstruction of the $h0l$ section of the reciprocal space obtained at the highest pressure reached.

RESULTS AND DISCUSSION

Phase stability of α-Cr_2O_3 at room temperature

In the present study we did not observe any signature of a phase transition or a structural instability of α-Cr_2O_3 up to 70.4(5) GPa at room temperature. Although some broadening of Bragg reflections does occur upon compression due to the development of stresses (see below), neither significant broadening or asymmetry, nor a splitting of individual reflections was detected. The volumetric and linear compressibility also do not reveal any discontinuity or non-monotonousness behavior (Table 1, Figs. 3 and 4).

These results are supported also by the independent experiment performed by Dera et al. (2011), and contradict with the conclusion of Shim et al. (2004) reporting that at room temperature Cr_2O_3 undergoes a displacive transition from a trigonal to a monoclinic phase at the pressure of around 14 GPa. This suggestion was based on a significant broadening of some of the X-ray diffraction reflections and the appearance of new (or splitting of existing) Raman modes. Similar observations in the Raman spectrum at similar pressure were made earlier by Mougin et al. (2001), however not associated with any changes in the X-ray diffraction pattern. This discrepancy between the current and the previous studies can be explained by the difference in the experimental conditions: a powder sample under non-hydrostatic conditions was used both by Shim et al. (2004) and by Mougin et al. (2001), whereas our study was conducted on single-crystalline material under quasi-hydrostatic conditions.

Bulk compressibility and equation of state

The observed P-V relation was fitted using an isothermal third-order Birch-Murhaghan equation of state (Poirier 2000), resulting in the bulk modulus K = 245(4) GPa and its first derivative K' = 3.6(2) (Table 2). V_0 value was fixed to 288.73 Å^3, as measured by Ovsyannikov and Dubrovinsky (2011) at ambient conditions on crystal from the same experimental bath.

The Cr_2O_3 compressibility (see Fig. 3 and Table 2) determined in this study is in a very good agreement with the results of Rekhi et al. (2000), Finger and Hazen (1980), and Dera et al. (2011). However, the calculated bulk modulus is significantly lower than those reported by Lewis and Drickamer (1966) and Mougin et al. (2001). Furthermore, lower values for both, bulk modulus and its pressure derivative, were obtained by Sato and Akimoto (1979). There is a clear trend: our results are very close to the results of those studies, which have been performed under the hydrostatic conditions and contradict with those held under non-hydrostatic conditions (using Ar, silicon oil, or no pressure medium at all). This conclusion demonstrates the importance of hydrostaticity for accurate compressibility and equation of state studies.

Linear compressibility and crystal structure

At pressures below ~20 GPa the compression of Cr_2O_3 appears to be almost isotropic, but at higher pressures it becomes

TABLE 1. P, V, lattice dimensions, and results of the structural refinement for Cr_2O_3 at room temperature and different pressures

P (GPa)	V (Å^3)	a (Å)	c (Å)	Atomic coordinates		U_{eq}(Cr)	U_{eq}(O)	Interatomic distances		$R1$ (%)	Total number of observed reflections	Number of unique reflections
				z(Cr)	x(O)			Cr-O(I), Å	Cr-O(II), Å			
0	288.73*	4.9530*	13.5884*	0.3475(1)*	0.3058(8)*	–	–					
8.1(1)	278.7(1)	4.8949(6)	13.432(2)	0.34730(4)	0.3080(5)	0.0031(4)	0.0041(7)	1.935(1)	1.995(2)	3.26	377	73
14.0(1)	273.6(1)	4.8645(6)	13.355(1)	0.34720(4)	0.3086(4)	0.0054(4)	0.0065(6)	1.924(1)	1.984(2)	2.90	458	72
20.4(2)	267.6(1)	4.8273(6)	13.264(2)	0.34700(5)	0.3105(5)	0.0074(6)	0.0093(8)	1.906(1)	1.976(2)	4.01	455	71
24.1(2)	265.8(1)	4.8152(6)	13.242(2)	0.34690(4)	0.3106(4)	0.0069(4)	0.008(1)	1.9021(9)	1.970(2)	2.80	446	70
29.6(2)	260.9(3)	4.785(2)	13.162(3)	0.34660(7)	0.3130(8)	0.0085(6)	0.012(1)	1.886(2)	1.965(3)	4.58	456	69
35.4(2)	256.7(3)	4.756(2)	13.109(3)	0.34630(5)	0.3143(5)	0.0089(7)	0.011(1)	1.875(1)	1.956(2)	3.80	449	68
39.7(2)	254.0(1)	4.737(1)	13.071(2)	0.34610(4)	0.3144(4)	0.0100(5)	0.0130(8)	1.869(1)	1.948(2)	3.96	449	65
44.8(2)	250.7(3)	4.714(2)	13.029(6)	0.34580(4)	0.3146(4)	0.0090(5)	0.0109(8)	1.8622(9)	1.938(2)	4.30	455	67
50.2(3)	247.1(4)	4.690(3)	12.972(6)	0.3455(5)	0.3161(5)	0.0105(6)	0.0142(9)	1.851(1)	1.932(2)	5.86	445	63
55.1(4)	244.8(3)	4.674(2)	12.941(5)	0.3452(5)	0.3169(6)	0.0097(4)	0.0125(8)	1.846(1)	1.926(2)	4.38	423	63
63.9(5)	238.9(6)	4.629(4)	12.880(9)	0.3447(6)	0.3205(6)	0.0117(6)	0.016(1)	1.826(1)	1.920(2)	5.50	434	67
70.4(5)	236.0(6)	4.605(4)	12.854(9)	0.3441(8)	0.3227(8)	0.0115(7)	0.015(1)	1.817(2)	1.916(3)	4.92	408	63

Notes: The x and y coordinates for chromium are fixed and equal zero. Furthermore, the following coordinates for the oxygen atoms are fixed: y(O) = 0 and z(O) = 0.25. The last column shows the number of the unique reflections used for the structural refinement at each pressure point.
* Data from Ovsyannikov and Dubrovinsky (2011).

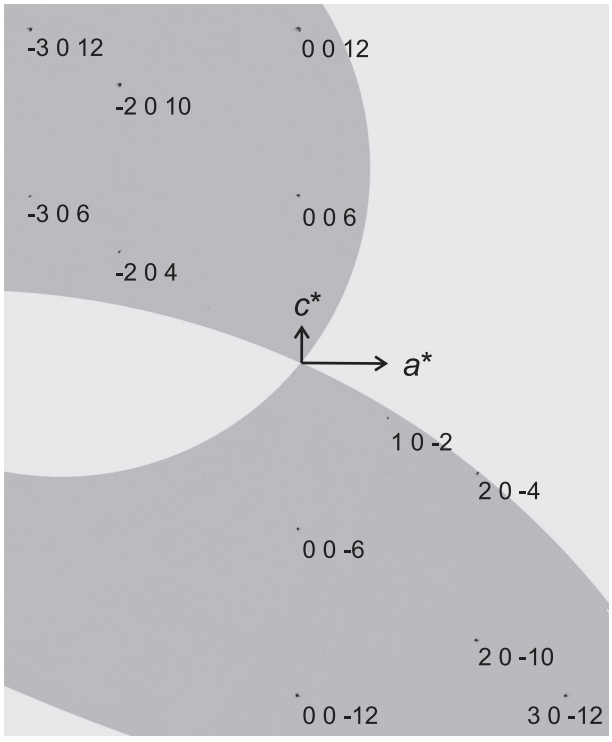

FIGURE 2. A reconstruction of the *h*0*l* reciprocal space section for Cr_2O_3 measured at 70.4(5) GPa.

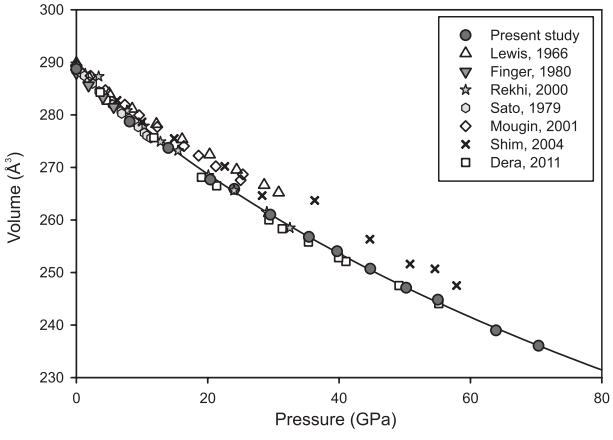

FIGURE 3. Compressibility of eskolaite Cr_2O_3. The data from the present study are shown in circles, from Lewis and Drickamer (1966) – triangles up, from Finger and Hazen (1980) – reversed triangles, from Rekhi et al. (2000) – squares, from Sato and Akimoto (1979) – hexagons, from Mougin et al. (2001) – diamonds, from Shim et al. (2004) – crosses, and from Dera et al. (2011) – stars. The solid line shows the calculated curve to our data.

clear that *a*-axis is more compressible than *c*-axis (see Fig. 4). However, the linear compressibility in both directions is monotonous within the uncertainty of measurements and can be perfectly described by the linear Birch-Murnaghan third-order equations (Poirier 2000).

The *c*/*a* ratio is an important indicator of the physical properties and the structural stability in the corundum-structured transition metal oxides. For the corundum structure with an ideal hexagonal close packing of oxygen, the *c*/*a* ratio is $2\sqrt{2} \approx 2.8284$. For the cation sublattice for any Cr ion there is one nearest neighbor in <001> direction, three nearest neighbors in the *a*-*b* plane at about 20% larger distance and 9 neighbors between hexagonal layers at ~60% larger distance. If Cr-Cr interactions are mostly repulsive, the *c*/*a* ratio is reduced relative to the ideal one – the situation observed not only for Cr_2O_3 (*c*/*a* ≈ 2.74), but also for Ti_2O_3 (*c*/*a* ≈ 2.65) (Newnham and de Haan 1962) and Fe_2O_3 (*c*/*a* ≈ 2.73) (Lewis and Drickamer 1966). The *c*/*a* ratio is also a good indicator of the electrical conductivity. Since metal-metal (M-M) pairs in the <001> direction do not form a continuous network, the in-plane interactions are responsible for the total conductivity. So the general trend is supposed to be an increasing conductivity with an increasing *c*/*a* ratio. This trend was demonstrated for pure and Cr-doped V_2O_3 (McWhan and Remeika 1970)—it is especially pronounced by the rapid jump of the *c*/*a* ratio when the oxide undergoes a metal to insulator transition.

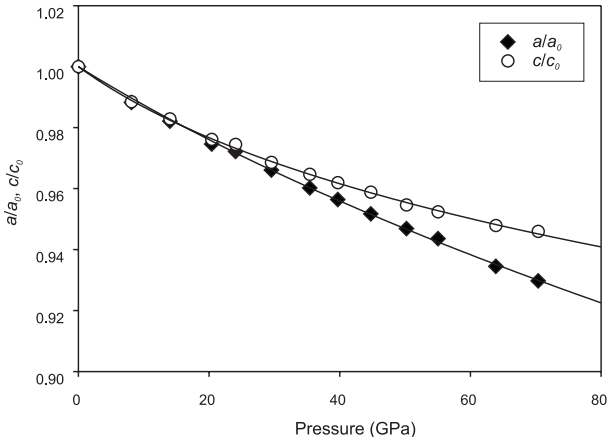

FIGURE 4. Relative compressibility of hexagonal *a* (diamonds) and *c* (circles) axes. Error bars are smaller than a symbol size. Lines are the linear third-order Birch-Murnaghan equations with the resulting effective parameters $K_0^a = 251(4)$ GPa, $K_0^{a\prime} = 2.5(1)$ and $K_0^c = 211(8)$, $K_0^{c\prime} = 8.4(7)$ for compressibility along the *a* and *c* axes, respectively.

According to our measurements, the *c*/*a* ratio in chromia gradually increases upon compression (thus probably indicating an increase of the electrical conductivity) from about 2.74 at ambient pressure to about 2.79 at 70.4 GPa (Fig. 5). It is important to note that the *c*/*a* ratio approaches the ideal value of 2.8284.

Due to symmetry constraints, there are only four independent parameters that fully define the crystal structure: lattice parameters *a* and *c*, chromium fractional coordinate *z* and oxygen fractional coordinate *x*. As is mentioned above, the crystal structure of chromia can be understood as a slightly distorted ideal closed-packed structure. Therefore, it is convenient to describe the deviations of crystal structure from ideal. Upon compression not only *c*/*a* ration shifts toward its ideal value, but also *z*(Cr) and *x*(O) approach 1/3 (see Table 1), a value for a perfect closed-packed structure. All other values of bond distances and angles, polyhedral distortions and volume, etc., could be calculated using these four independent parameters. For example, the compressibility of the different oxygen-oxygen distances is

TABLE 2. Calculated and reported values of bulk modulus, its pressure derivative, and volume of Cr_2O_3

	Lewis and Drickamer (1966)	Sato and Akimoto (1979)	Finger and Hazen (1980)	Rekhi et al. (2000)	Mougin et al. (2001)	Dera et al. (2011)	Present study
Isothermal bulk modulus (K_T) (GPa)	272	231	238	240	259	220(4)	245(4)
Pressure derivative (K_T')	5.5	2.0	4 (fixed)	3.5	5.0	4.7(2)	3.6(2)
Volume (V_0) (Å^3)	289.82	–	287.9	289	–	288.6(2)	288.73*

* Data from Ovsyannikov and Dubrovinsky (2011).

different, where the contraction is higher for the longer bonds (Fig. 6). The distortion of CrO_6 octahedron therefore decreases with increasing pressure, and the relative difference between the longest and the shortest O-O distance decreases from 3.2% at ambient pressure to about 1.2% at 70 GPa. Both, bulk compressibility and structural parameters of Cr_2O_3 obtained in this study are in a remarkable agreement with the results obtained by Dera et al. (2011)—see Figures 3, 5, and 6.

From the point of view of classical crystallography, the main reason for the structural distortion of the corundum type structure in the repulsion force between highly charged cations sharing a common octahedron face. Upon compression, this repulsion probably becomes weaker [z(Cr) decreases from 0.3475(1) to 0.3441(8)], and the whole structure converges to an ideal closed-packed one. This is consistent with the reported pressure-induced increase in the chemical bonding covalency in Cr_2O_3 (Tkacz-Smiech et al. 2000).

Non-hydrostatic stresses and corresponding crystal strains

Although neon is considered as a quasi-hydrostatic pressure medium, in reality it solidifies above ~4.7 GPa at room temperature (Vos et al. 1991), therefore certain non-hydrostatic stresses should exist inside a sample chamber at higher pressures. Although we do not have any direct probe of the non-hydrostatic stresses, we can analyze strains of the sample crystal in more detail. In general, a non-uniform stress results in a non-uniform strain in the crystal. If the stress is spherically anisotropic, it should result in systematic d-spacing shifts depending on the orientation of the crystal relative to the stress tensor. In particular, since a diamond-anvil cell possesses an axial symmetry with a loading direction normal to the diamond culet surface, a systematic deviation of the observed d-spacing as a function of the angle ψ between the DAC loading axis and plane normal is expected (Singh et al. 1998). If we note deviation of the interatomic plane distance from a hydrostatic pressure value as $\Delta d/d$, the dependence is:

$$\frac{\Delta d}{d} = Q(hkl)[1-3\cos^2\psi] \quad (1)$$

where $Q(hkl)$ is an orientation-dependent distortion parameter. For rough estimation we can assume that

$$Q(hkl) \approx \frac{t}{3G} \quad (2)$$

where G is the aggregate shear modulus, and t is the difference between axial and radial principal stresses on the sample.

We performed this kind of analysis for the highest pressure. A total of 117 individual reflections (including symmetry equiva-

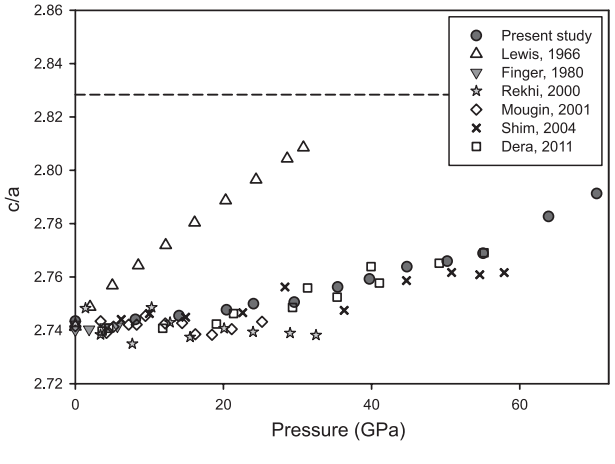

FIGURE 5. The c/a ratio of chromia as a function of pressure. The data of the present study are shown as circles, from Lewis and Drickamer (1966) – triangles up, from Finger and Hazen (1980) – reversed triangles, from Rekhi et al. (2000) – squares, from Mougin et al. (2001) – diamonds, from Shim et al. (2004) – crosses, and from Dera et al. (2011) – stars. The dashed line shows the ideal value of the c/a ratio (~2.8284).

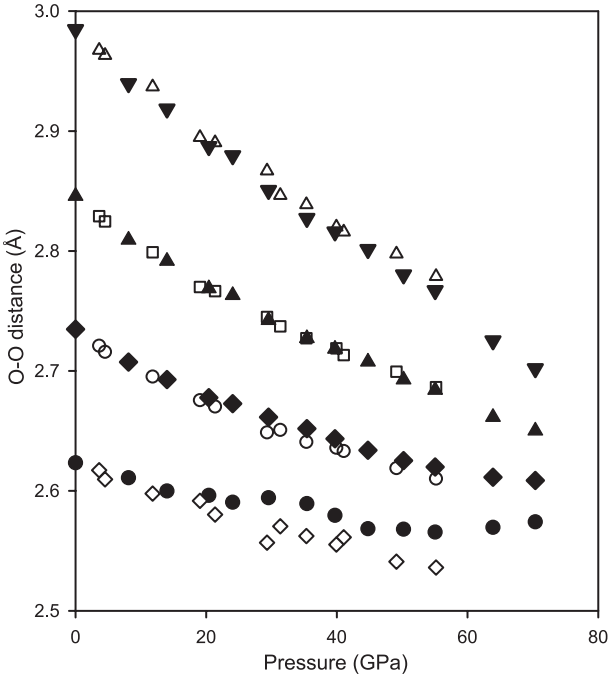

FIGURE 6. O-O distances along the 12 edges of the CrO_6 octahedron (the uncertainties are within the symbol sizes). The shortest distances are the three bonds belonging to the shared face; the intermediate three distances are the shared edges; and the remaining longest distances are non-shared edges of the CrO_6 octahedron. Open symbols present data from Dera et al. (2011), filled symbols – the data from the present study.

lents) were observed, and for every single reflection a *d*-spacing and $(1 - 3\cos^2\psi)$ were calculated (Fig. 7). No systematic trend was observed in the data, even in the particular (*hkl*) planes, and we can state that there is no systematic trend in $\Delta d/d$ larger than 0.0005 over the available angular range.

Although we have no experimental information on the shear modulus of eskolaite at 70 GPa, we can make an estimation based on an ambient pressure value of 162 GPa (Frantsevich et al. 1982) and pressure derivative dG/dP of 2, which is the typical value for dense oxides (see, for example, Hofmeister and Mao 2003). An estimated value for the shear modulus of Cr_2O_3 at 70 GPa is probably not more than 310 GPa. In this case, according to the Equations 1 and 2, we can conclude that the uniaxial stress at the maximum pressure of 70 GPa does not exceed 0.25 GPa in our experiment.

In addition to the uniaxial stress there is another type of non-uniform stress associated with the non-hydrostaticity of the pressure medium, namely, the non-uniform stress distribution inside the sample volume (pressure gradients). Pressure gradients reveal themselves as microstrains that result in a systematic broadening of the X-ray diffraction peaks. This kind of microstrain (often denoted as mean tensile strain η) can be extracted by analyzing the integral breadth β of reflections as a function of diffraction angle θ (Stokes and Wilson 1944). At every pressure point for each observed X-ray diffraction reflections an integral breadth β was calculated assuming a Gaussian peak profile (for a pure Gaussian function $\beta = \sigma\sqrt{2\pi}$). The resulting values indeed show a linear dependence between $4\times\sin(\theta)$ and $\beta\times\cos(\theta)$ (Fig. 8, inset), and the slope of this line gives the mean tensile strain h (Fig. 8). The intercept of this line with the y-axis is a convolution of the instrumental resolution function and an effective crystallite size. In the present study we do not observe any increase of the intercept, indicating that the effective crystalline size (or the coherent scattering volume) remains constant and no significant development of the crystal mosaicity occurs upon compression.

The mean tensile strain increases up to about 1.4×10^{-3} at the highest pressure reached (see Fig. 8), which roughly corresponds to a compressional stress of the order of 0.7 GPa, estimated using the equation of state reported here. Even if all the tensile strain arises from the pressure gradients, those gradients are comparable with the uncertainty of the pressure determination.

With the diffraction geometry used (omega-scans and area-sensitive detector), in principal each diffraction peak can be characterized with three independent angles profiles: 2θ (Bragg angle between incident and diffracted beams), ω (angle of the DAC rotation around vertical axis), and μ = the angle between a vertical plane and a diffraction plane (a plane containing incident and diffracted beams). Peaks broadening in θ are analyzed above; ω in our experiment does not have enough resolution to extract peak profiles (diffraction frames were collected with 0.5° steps in ω, which is typical for such kinds of measurements), but μ-profiles of individual peaks can be extracted with about the same resolution as the 2θ-profiles. This angle is also called a mosaicity angle, because in the unstressed sample peak width in μ is a measure of crystal mosaicity. The width of a diffraction peak in μ-angle reflects a distribution of interatomic planes normal in the direction perpendicular to the diffraction plane. When a single-crystal breaks into a series of slightly misoriented crystallites, a diffraction peak broadens in μ, and, in the extreme case of randomly oriented powder, a μ-width becomes a full 360° continuum and a single-crystal diffraction spot transforms into a Debye-Scherrer diffraction ring. The μ-profiles of each diffraction peak of Cr_2O_3 were extracted for each pressure assuming the Gaussian shape of diffraction peaks. No systematic variations of μ full-width at half maximum (FWHM) neither with the angle ψ between the DAC loading axis and the diffraction plane normal, nor with the crystallographic direction have been observed. An average value of the Gaussian standard deviation for all peaks as a function of pressure is shown in Figure 9. As can be seen, this parameter also increases upon compression from 0.05 to about 0.12 at the highest pressure. This increase, however, cannot be explained as an increase of the crystal mosaicity, because we

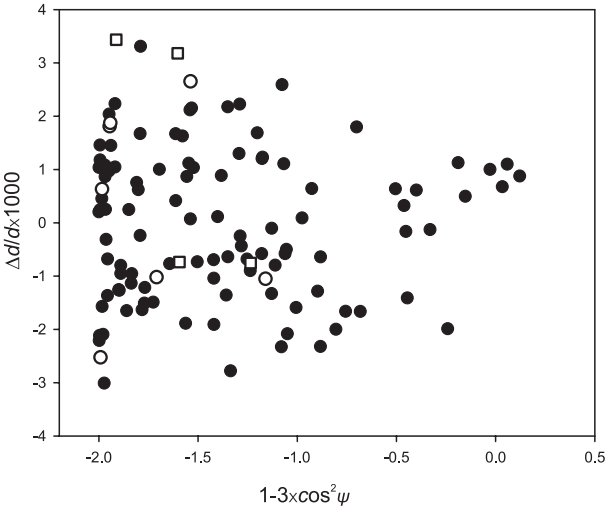

FIGURE 7. Relative deviations of *d*-spacing as a function of $(1 - 3\cos^2\psi)$. Open circles show the deviations for the reflections of the (116) plane, and the open squares are for the (113) plane symmetry equivalents.

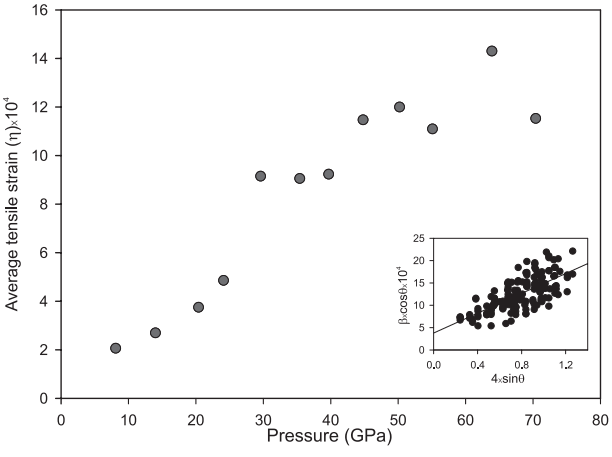

FIGURE 8. Measured average tensile strain in Cr_2O_3 crystal as a function of pressure. Insert shows a typical Williamson-Hall plot for P = 35.4(2) GPa. β is the integral width of a reflection and θ is the diffraction angle.

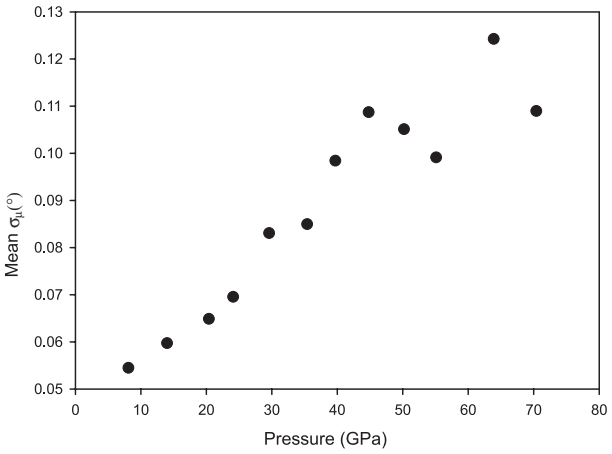

FIGURE 9. An average value of μ Gaussian standard deviation as a function of pressure.

did not observe any decrease of the effective crystalline size from the microstrain analysis. An alternative explanation of the μ width increase is an elastic bending of the crystal in the direction, perpendicular to the diffraction normal. To make an accurate stress-strain calculation of this kind of bending one needs to know a full elastic tensor and the exact shape of the single crystal. However a semi-qualitative estimation can be made for the highest pressure in the isotropic assumption using the abovementioned values for the bulk and shear moduli, and approximating an X-ray probed-part of the crystal as a cuboid of $15 \times 15 \times 15$ μm^3. This estimation gives an average pure bending component of the stress tensor of ~0.3 GPa. This value is quite close to the compressional stress variation of ~0.5 GPa estimated from the 2θ profiles. Therefore we can conclude that in the neon pressure medium at about 70 GPa stress tensor deviates from the uniform (hydrostatic) by about 1% only.

CONCLUDING REMARKS

We determined an evolution of the Cr_2O_3 crystal structure at pressures below 70.4 GPa under quasi-hydrostatic conditions and verified that there is no pressure induced structural phase transition in the whole range of pressures studied. This conclusion coincides with the results obtained earlier by Rekhi et al. (2000) and by Dera et al. (2011), however it contradicts with some other studies (Minomura and Drickamer 1963; Mougin et al. 2001; Shim et al. 2004). This controversy might be explained with the differences in hydrostaticity between different experiments. The fact that a distortional phase transition may occur under non-hydrostatic stress and be absent under a quasi-hydrostatic conditions is important. There is a good example of $(Mg_{0.8}Fe_{0.2})O$ mixed oxide, where a distortional cubic to rhombohedral transition was observed only under non-hydrostatic compression without a pressure transmitting medium (Kantor et al. 2006). Comparing our observations with the data available in the literature, we suggest that stresses induced by non-hydrostatic conditions should expand the *P-T* thermodynamic space of Cr_2O_3 and probably of many other materials, and thus may result not only in subtle effects like shifting of phase boundaries, but also in the creation of new phase fields, which should not exist under purely hydrostatic pressure.

A detailed analysis of diffraction peaks profiles demonstrates that non-hydrostatic components of the stress tensor do not exceed 1% (well below 1 GPa) at 70 GPa when neon gas is used as a pressure-transmitting medium.

ACKNOWLEDGMENTS

We acknowledge the ESRF for the provision of the beam-time and for supporting the visiting scientist activity of M.M. We thank S. Ovsyannikov for providing us the single crystal of Cr_2O_3. We also acknowledge the financial support by German BMDF and DFG funds.

REFERENCES CITED

Boehler, R., and Hantsetters, K. (2004) New anvil designs in diamond-cells. High Pressure Research, 24, 391–396.

Dera, P., Lavina, B., Meng, Y., and Prakapenka, V.P. (2011) Structural and electronic evolution of Cr_2O_3 on compression to 55 GPa. Journal of Solid State Chemistry, 184, 3040–3049.

Dobin, A.Y., Duan, W., and Wentzcovitch, R.M. (2000) Magnetostructural effects and phase transition in Cr_2O_3 under pressure. Physical Review B, 62, 11997–12000.

Dubrovinsky, L., Boffa-Ballaran, T., Glazyrin, K., Kurnosov, A., Frost, D., Merlini, M., Hanfland, M., Prakapenka, V., Schouwink, P., Pippinger, T., and Dubrovinskaia, N. (2010) Single-crystal X-ray diffraction at megabar pressures and temperatures of thousands of degrees. High Pressure Research, 30, 620–633.

Fei, Y., Ricolleau, A., Frank, M., Mibe, K., Shen, G., and Prakapenka, V. (2007) Towards an internally consistent pressure scale. Proceedings of the National Academy of Sciences, 104, 9182–9186.

Finger, L.W., and Hazen, R.M. (1980) Crystal structure and isothermal compression of Fe_2O_3, Cr_2O_3, and V_2O_3 to 50 Kbars. Journal of Applied Physics, 51, 5362–5367.

Frantsevich, I.N., Voronov, F.F., and Bokuta, S.A. (1982) In I.N. Frantsevich, Ed., Elastic Constants and Elastic Moduli of Metals and Insulators: Handbook, p. 60–180. Naukova Dumka, Kiev.

Hofmeister, A.M.; and Mao, H.K. (2003) Pressure derivatives of shear and bulk moduli from the thermal Gruneisen parameter and volume-pressure data. Geochimica et Cosmochimica Acta, 67, 1215–1235.

Kantor, I.Yu., Dubrovinsky, L.S., McCammon, C., Kantor, A.P., Pascarelli, S., Aquilanti, G., Crichton, W., Mattesini, M., Ahuja, R., Almeida, J., Urusov, V. (2006) Pressure-induced phase transition in $Mg_{0.8}Fe_{0.2}O$ ferropericlase. Physical and Chemistry of Minerals, 33, 35–44.

Lewis, G.K., and Drickamer, H.G. (1966) Effect of high pressure on the lattice parameters of Cr_2O_3 and a-Fe_2O_3. Journal of Chemistry and Physics, 45, 224–226.

Mao, H.K., Xu, J.A., and Bell, P.M. (1986) Calibration of the ruby pressure gauge to 800 kbar under quasihydrostatic conditions. Journal of Geophysical Research, 91, 4673–4676.

McWhan, D.B., and Remeika, J.P. (1970) Metal-Insulator Transition in $(V_{1-x}Cr_x)_2O_3$. Physical Review B, 2, 3734–3750.

Merlini, M., Crichton, W.A., and Hanfland, M. (2012) $CaCO_3$-III and $CaCO_3$-VI, high-pressure polymorphs of calcite: Possible host structures for carbon in the Earth's mantle. Earth and Planetary Science Letters, 333–334, 265–271, DOI: 10.1016/j.epsl.2012.04.036.

Minomura, S., and Drickamer, H.G. (1963) Effect of pressure on the electrical resistance of some transition metal oxides and sulfides. Journal of Applied Physics, 34, 3043–3048.

Mougin, J., Le Bihan, T., and Lucazeau, G. (2001) High-pressure study of Cr_2O_3 obtained by high-temperature oxidation by X-ray diffraction and Raman spectroscopy. Journal of Physics and Chemistry of Solids, 62, 553–563.

Newnham, R.E., and de Haan, Y.M. (1962) Refinement of the α-Al_2O_3, Ti_2O_3, V_2O_3 and Cr_2O_3 structures. Zeitschrift für Kristallographie, 117, 235–237.

Ovsyannikov, S., and Dubrovinsky, L. (2011) High-pressure high-temperature synthesis of Cr_2O_3 and Ga_2O_3. High Pressure Research, 31, 23–29.

Oxford Diffraction (2006) CrysAlis RED, Oxford Diffraction Ltd, Abingdon, Oxfordshire, U.K.

Poirier, J.-P. (2000) Introduction to the Physics of the Earth's Interior (2nd edition). 326 p. Cambridge University Press, U.K.

Rekhi, S., Dubrovinsky, L.S., Ahuja, R., Saxena, S.K., and Johansson, B. (2000) Experimental and theoretical investigations on eskolaite (Cr_2O_3) at high pressures. Journal of Alloys and Compounds, 302, 16–20.

Sato, Y., and Akimoto, S. (1979) Hydrostatic compression of four corundum-type compounds: α-Al_2O_3, V_2O_3, Cr_2O_3, and α-Fe_2O_3. Journal of Applied Physics, 50, 5285–5291.

Sheldrick, G.M. (2008) A short history of SHELX. Acta Crystallographica A, 64, 112–122.

Shim, S.-H., Duffy, T.S., Jeanloz, R., Yoo, C.-S., and Iota, V. (2004) Raman

spectroscopy and X-ray diffraction of phase transitions in Cr_2O_3 to 61 GPa. Physical Review B, 69, 144107.
Singh, A.K., Mao, H-K., Shu, J., and Hemley, R.J. (1998) Estimation of single-crystal elastic moduli from polycrystalline X-ray diffraction at high pressure: Application to FeO and Iron. Physical Review Letters, 80, 2157–2160.
Stokes, A.R., and Wilson, A.J.C. (1944) The diffraction of X-rays by distorted crystal aggregates-I. Proceedings of the Physical Society, 56, 174–181.
Tkacz-Smiech, K., Kolezynski, A., and Ptak, W.S. (2000) Pauling's electrostatic rule for partially covalent/partially ionic crystals. Journal of the Physics and Chemistry of Solids, 61, 1847–1853.
Vos, W.L., Schouten, J.A., Young, D.A., and Ross, M. (1991) The melting curve of neon at high pressure. Journal of Chemical Physics, 94, 3835–3838.

Manuscript received January 12, 2012
Manuscript accepted June 26, 2012
Manuscript handled by G. Diego Gatta